EPJ Web of Conferences **17**, 08003 (2011)
DOI: 10.1051/epjconf/20111708003

(Multi-)nucleon transfer in the reactions ^{16}O,^{32}S+^{208}Pb

M. Evers[1,a], M. Dasgupta[1], D. J. Hinde[1], and C. Simenel[2]

[1] Department of Nuclear Physics, Research School of Physics and Engineering, The Australian National University, Canberra, ACT 0200, Australia
[2] CEA, Centre de Saclay, IRFU/Service de Physique Nucleaire F-91191 Gif-sur-Yvette, France

Abstract. A detailed analysis of the projectile-like fragments detected at backward angles in the reactions ^{16}O,^{32}S+^{208}Pb at energies below the fusion barrier is presented. Excitation functions corresponding to nucleon transfer with $\Delta Z = 1$ and $\Delta Z = 2$ were extracted, indicating surprisingly large absolute probabilities at sub-barrier energies. A comparison of $2p$ transfer probabilities with time-dependent Hartree-Fock calculations suggests strong pairing correlations between the two protons. Excitation energies in the projectile-like fragments $\sim$ 15 MeV and $\sim$ 25 MeV for the ^{16}O and ^{32}S-induced reactions, respectively, indicate the population of highly excited states in the residual nuclei. A comparison with expected optimum Q-values suggests large losses in kinetic energy of the projectile-like fragments. These highly inelastic (large excitation energies) and complex (correlated few-nucleon transfer) processes may be closely related to the depletion of fusion through tunnelling at sub-barrier energies.

1 Introduction

A major question in near-barrier reactions is to explain the physical mechanisms causing the suppression of fusion, seen both at deep sub-barrier and at above-barrier energies in reactions of heavy nuclei [1–3]. Extrapolations of fusion probabilities to energies typical for astrophysical scenarios, show an extremely large spread (up to 40 orders of magnitude), based on different phenomenological models [20,3,21].

A process believed to be closely related to fusion suppression is the dissipation of kinetic energy through deep inelastic collisions (DIC) [1,4], which become important with increasing nuclear overlap at energies near and above the fusion barrier energy. The importance and systematics of (multi-) nucleon transfer processes in DIC at energies well above the fusion barrier has been discussed in a recent review [5]. Transfer processes that lead to high excitation energies in the residual nuclei were suggested as a key to understanding the suppression of fusion through the onset of irreversible dissipative processes [1,19].

In this work, the question is addressed whether these concepts can also explain the suppression of fusion through tunnelling. In this context and using the reactions ^{16}O,^{32}S+^{208}Pb, (i) the significance of transfer processes in nuclear collisions at energies *well below* the fusion barrier is investigated, and (ii) the details and underlying mechanisms of these transfer processes are explored.

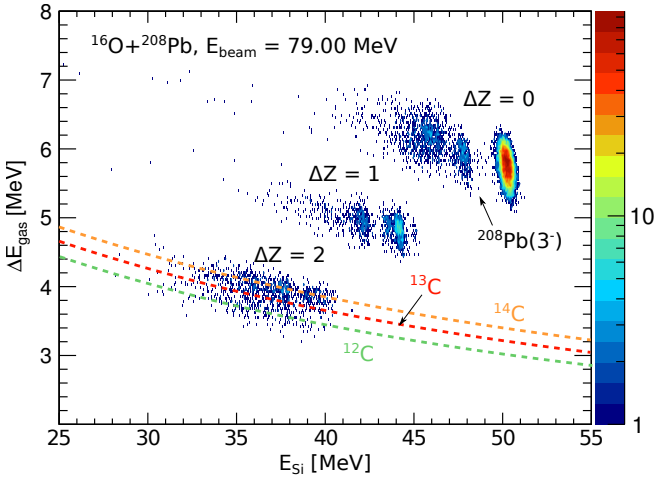

Fig. 1. (Color online) Two dimensional $\Delta E - E$ spectrum for the reaction ^{16}O+^{208}Pb at the indicated beam energy, corresponding to $E_{c.m.}/V_B = 0.98$. The three different regions indicating $\Delta Z = 0, 1, 2$ transfer are labeled. Calculated energy loss curves (dashed curves) for ^{14}C, ^{13}C and ^{12}C are shown.

2 Measurements

Measurements were carried out using the 14UD electrostatic accelerator of the Heavy-Ion Accelerator Facility at The Australian National University (ANU). Beams of ^{16}O and ^{32}S were incident on a ^{208}PbS target with a thickness of 100 μg/cm^2, evaporated onto a 15 μg/cm^2 C backing. A detector telescope consisting of a Propane gas ionization chamber and a Si detector located at a backward angle

[a] e-mail: maurits.evers@anu.edu.au

of $\theta_{\rm lab} = 162°$ was used to record the energy and energy loss of the back-scattered projectile-like fragments (PLFs). Two Si monitors positioned at ±30° were used to normalize the back-scattered events to the Rutherford cross section. A typical two dimensional spectrum for a measurement of the reaction ^{16}O+^{208}Pb at a beam energy corresponding to $E_{c.m.}/V_B = 0.98$ is shown in Fig. 1. The three distinct regions correspond to oxygen, nitrogen and carbon PLFs, which are associated with the transfer of $\Delta Z = 0$, 1 and 2 units of charge. The main peak at $E_{\rm Si} \sim 50$ MeV corresponds to elastically scattered ^{16}O particles, the smaller peak at $E_{\rm Si} \sim 48$ MeV is associated with the excitation of the lowest 3^- excited state in ^{208}Pb at an excitation energy of 2.615 MeV. Events resulting from the transfer of three or more charged nucleons ($\Delta Z \geq 3$) are not observed for measurements at sub-barrier energy. Energy spectra for measurements of the reaction ^{32}S+^{208}Pb show similar features.

3 Transfer excitation functions

Transfer probabilities for processes with different ΔZ were extracted by gating on the particular region of interest in the $\Delta E - E$ spectra, and normalizing the number of events to the total number of counts in the two forward angle monitor detectors. Overall normalization of the probabilities was achieved using the total quasi-elastic excitation function, following the procedure detailed in Ref. [6].

3.1 Absolute transfer probabilities for processes with $\Delta Z = 1$ and $\Delta Z = 2$ in the reaction ^{16}O+^{208}Pb

For the reaction ^{16}O+^{208}Pb, transfer probabilities for $\Delta Z = 1$ (nitrogen PLFs) and $\Delta Z = 2$ (carbon PLFs) are shown in Fig. 2 by the filled squares and diamonds, respectively. The transfer probabilities are plotted as a function of the distance of closest approach assuming a Coulomb trajectory [7]

$$r_{\rm min} = \frac{Z_p Z_t e^2}{4\pi\epsilon_0} \frac{1}{2E_{c.m.}} \left(1 + {\rm cosec}\, \frac{\theta_{c.m.}}{2}\right), \qquad (1)$$

where Z_p, Z_t are the atomic numbers of projectile and target nucleus, and $E_{c.m.}$ and $\theta_{c.m.}$ are the energy and scattering angle in the centre-of-mass frame, respectively. The absolute probabilities at an energy around the fusion barrier agree very well with previous measurements [8] at $E_{c.m.}/V_B \sim 1.0$, which are shown by the large open square and diamond symbols for the nitrogen and carbon PLFs, respectively. Earlier measurements at the ANU of the nitrogen and carbon PLFs from Ref. [9] are shown by the smaller open squares and diamonds, respectively, and also show excellent agreement. Neither measurements however allowed a separation in mass of the PLFs.

The well separated reaction Q-values for $\Delta Z = 1$ transfer processes in the reaction ^{16}O+^{208}Pb allow the identification of the predominant contribution to the $\Delta Z = 1$ events with the transfer of one proton ($1p$-stripping). An

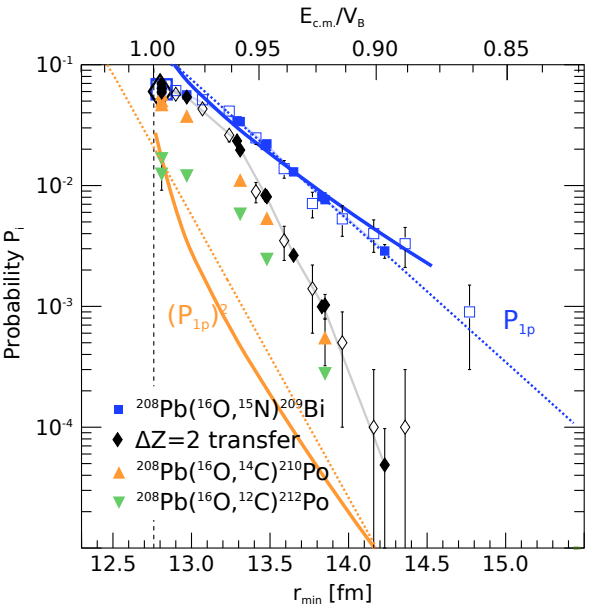

Fig. 2. (Color online) Transfer probabilities for the indicated transfer processes as a function of the distance of closest approach, see Eq. (1). The asymptotic behaviour for $1p$ transfer and sequential $2p$ transfer are shown by the dotted straight lines. TDHF calculations for $1p$ and $2p$ transfer are shown by the solid blue and orange curves. The vertical dashed line indicates the barrier position. The large open square and diamond at $E_{c.m.}/V_B \sim 1.0$ are the measurements for N (blue) and C PLFs (black) from Videbaek et al. [8]. The smaller open squares and diamonds are the measurements for N (blue) and C PLFs (black) from Timmers [9].

isotopic mass separation of the $\Delta Z = 2$ carbon fragments was possible using the calculated energy loss curves for different carbon isotopes and determining the contributions from ^{12}C, ^{13}C and ^{14}C to the integrated $\Delta Z = 2$ counts. Extracted transfer probabilities for the two processes $2p$-stripping ^{208}Pb(^{16}O,^{14}C)^{210}Bi and α-particle stripping ^{208}Pb(^{16}O,^{12}C)^{212}Bi are shown in Fig. 2 by the orange and green triangles, respectively. Transfer probabilities for the $2p1n$-stripping process ^{208}Pb(^{16}O,^{13}C)^{211}Bi are not shown since they are at least 10 times smaller than those for α-particle transfer. Contrary to what was commonly assumed [10–13], at sub-barrier energies $2p$ transfer (orange triangles in Fig. 2) is the dominant process. α-particle transfer probabilities (green triangles) are smaller by a factor of $\sim 2-3$ compared to that of $2p$ transfer. The difference in probabilities between $2p$ and α transfer increases with increasing beam energy, and is largest at $E_{c.m.}/V_B \sim 1.0$.

Since the unambiguous identification of the dominant contribution to the $\Delta Z = 2$ transfer events depended critically on the accuracy of the energy loss calculations and energy calibration of the detector, additional measurements with beams of ^{12,13}C using the same experiment were performed. Scattering them from a thick tantalum target provided empirical energy loss curves for the gas-Si detector, and confirmed the validity of the energy loss calculations and thus the identification of the predominant contribution to the $\Delta Z = 2$ events with the transfer of two protons.

For the reaction ^{32}S+^{208}Pb, measurements also indicate that $2p$-stripping is the dominant $\Delta Z = 2$ transfer process, which was confirmed independently by performing measurements with beams of ^{30}Si using the same experiment.

3.2 Time-dependent Hartree-Fock calculations

TDHF calculations for the reaction ^{16}O+^{208}Pb using the TDHF3D code developed by P. Bonche et al. were performed, using the SLy4*d* Skyrme parametrization [14]. It uses a full Skyrme type interaction, described in detail in Ref. [15], and allows the calculation of transfer excitation functions for $1p$ and $2p$ transfer using particle number projection techniques on the PLFs. Since TDHF calculations are based on an independent particle picture, calculated $2p$ transfer probabilities imply sequential transfer of two uncorrelated protons.

Results for the $1p$ and $2p$ transfer probabilities based on TDHF calculations carried out by C. Simenel [22] are shown by the solid blue and orange curves in Fig. 2. All TDHF results overestimated the extracted transfer probabilities, and thus *all* TDHF transfer probabilities ($1p$ and $2p$) were scaled by a factor of 0.43 to match the experimental $1p$ transfer probabilities in the interval $0.9 < E_{c.m.}/V_B < 1.0$ in which absorptive processes are negligible. The energy dependence of the TDHF calculations agree with the $1p$ transfer probabilities. The measured $2p$ probabilities are much higher than the TDHF calculations (solid orange curve in Fig. 2), indicating that in reality there is a strong pairing correlation between the two protons, which leads to the enhanced $2p$ transfer probabilities. The TDHF calculations for $2p$ transfer are in close agreement with the experimentally deduced sequential $2p$ transfer probabilities $(P_{1p})^2$ (shown by the dotted orange line in Fig. 2), where P_{1p} is the experimentally measured $1p$ transfer probability.

Overall, the agreement between TDHF calculations and the energy dependence of the extracted transfer probabilities for $1n$ and $1p$ transfer at energies below the fusion barrier is good. Absolute probabilities of all TDHF calculations are however too large by a factor of ~ 2.3. The calculated $2p$ transfer probabilities under-predict the extracted $2p$ transfer probabilities and therefore independently confirm a strong pairing correlation of the two protons in the observed $2p$ transfer probabilities.

4 Excitation energies

Excitation energies for the $\Delta Z = 1$ and $\Delta Z = 2$ PLFs were determined using the corresponding dominant transfer reactions leaving the residual nuclei in their ground states as the reference processes. Where populated, the ground-state transfers provided a good check of the energy calibration. From the excitation energy spectra, the differential transfer probabilities dP/dE_x were determined. Fig. 3 shows dP/dE_x as a function of E_x and the energy above the fusion barrier energy $E_{c.m.}-V_B$ for the PLFs following $2p$ and α-particle transfer in the ^{16}O- (top panel) and ^{32}S-induced reactions (bottom panel). The resulting contour plots give a complete picture of the dynamics of the PLFs as a function of energy.

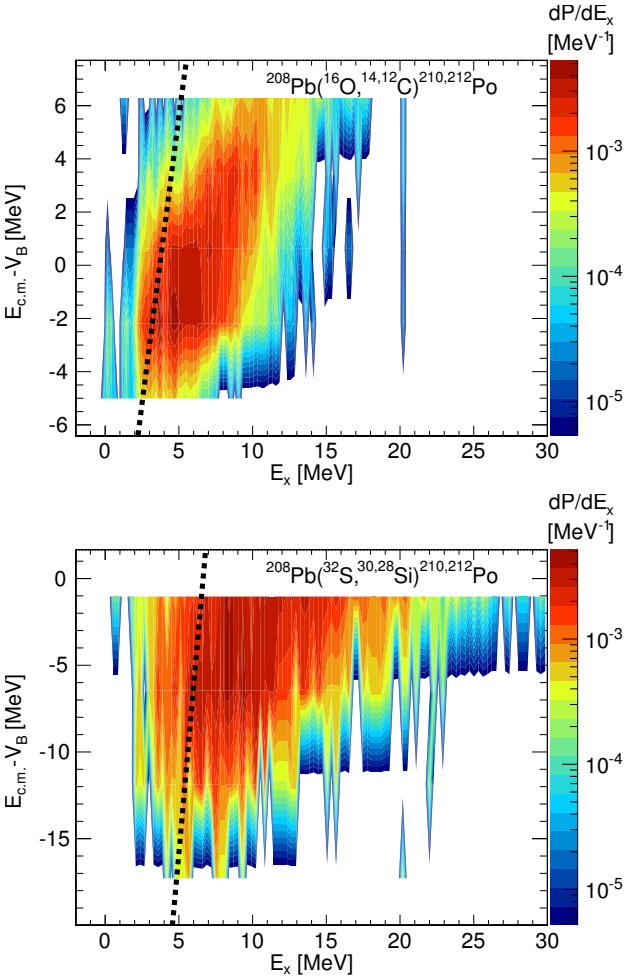

Fig. 3. Contour plot of the differential transfer probabilities dP/dE_x as a function of the excitation energy E_x (i.e. kinetic energy loss taking into account the specific reaction Q value) of the PLFs (abscissa) and energy above the fusion barrier energy $E_{c.m.} - V_B$ (ordinate) for the $\Delta Z = 2$ transfer processes ($2p$, α transfer) in the reactions ^{16}O+^{208}Pb (top panel) and ^{32}S+^{208}Pb (bottom panel). The dotted black lines indicate the optimum excitation energies $E_x^{\rm opt}$ defined in Eq. (2).

Excitation energies are generally higher for the ^{32}S-induced reactions than for the ^{16}O case. Both reactions show the population of highly excited states at energies well below the fusion barrier. At an energy ~ 5 MeV below the barrier, excitation energies of ~ 15 MeV are observed for the ^{16}O-induced reaction and ~ 25 MeV for the ^{32}S-induced reaction, respectively.

4.1 Optimum Q-values

It is possible to define an optimum excitation energy as

$$E_x^{\rm opt} = Q_{\rm gg} - Q_{\rm opt}(E_{c.m.}), \qquad (2)$$

where $Q_{\rm gg}$ and $Q_{\rm opt}$ are the ground state and (energy-dependent) optimum Q-value of the transfer reaction re-

spectively, see e.g. Refs. [16–18]. In a simplified picture (ignoring recoil effects) $Q_{\rm opt}$ is given by

$$Q_{\rm opt} = E_{c.m.}\left(\frac{Z'_pZ'_t}{Z_pZ_t} - 1\right), \qquad (3)$$

where Z'_p, Z'_t are the atomic numbers of the projectile- and target-like nuclei after the transfer. The excitation energies in Eq. (2) correspond to the *optimum* excitation energies based on a semi-classical treatment of transfer reactions by matching the classical trajectories of the projectile nucleus before and after the transfer. In Fig. 3, Eq. (2) has been expressed in terms of E_x, which corresponds to the kinetic energy loss of the PLF due to excitations of the projectile-like or target-like nucleus, taking into the account the specific reaction Q value due to,

$$(E_{c.m.} - V_B) = C_0 - C_1E_x^{\rm opt}\ , \qquad (2')$$

which corresponds to diagonal lines with slope C_1 and offset C_0, indicated by the dotted black lines. In the absence of processes leading to energy loss, the centroids, corresponding to the maximum of the transfer probabilities dP/dE_x shown by the contours in Fig. 3, are therefore expected to follow this slope. Dissipative and irreversible processes such as the evaporation of nucleons should lead to a loss in kinetic energy of the PLFs, which would manifest itself in a deviation of the differential transfer probabilities centroid from the diagonal lines representing Eq. (2) as a function of $E_{c.m.} - V_B$. As can be seen from Fig. 3, there is a significant contribution of the differential transfer probabilities located at excitation energies *higher* than the optimum excitation energy, suggesting that dissipative processes play an important role already at these sub-barrier energies.

5 Conclusion

In conclusion, the following results were obtained from a detailed analysis of the projectile-like fragments detected at a backward angle in the reactions ^{16}O,^{32}S+^{208}Pb:

1. Transfer of two protons ($2p$-stripping) in the reactions ^{16}O,^{32}S+^{208}Pb occurs with a significant probability already at energies well below the fusion barrier. $2p$ transfer is the predominant $\Delta Z = 2$ transfer process, with absolute probabilities being $\sim 2-3$ times larger than those for α-particle transfer.
2. The transfer excitation functions for $2p$ transfer in ^{16}O+^{208}Pb suggest a strong pairing correlation of the two transferred protons. This is supported by TDHF calculations based on the independent particle picture.
3. The residual nuclei following $2p$ and α-particle transfer are left in highly excited states, with excitation energies ~ 15 MeV and ~ 25 MeV for the ^{16}O- and ^{32}S-induced PLFs, respectively. A comparison with $Q_{\rm opt}$ calculations show projectile-like fragments with larger kinetic energy losses than expected based on these semi-classical considerations. This suggests that dissipative and irreversible processes play an important role already at energies well below the fusion barrier.

These considerations strongly support the idea that few-nucleon transfer triggers the onset of dissipative and irreversible processes in the collision of nuclei already at energies well-below the fusion barrier, ultimately adversely affecting the probability of the nuclei to fuse in the tunnelling regime.

References

1. J. Newton *et al.*, Phys. Rev. C **70**, (2004) 024605.
2. M. Dasgupta *et al.*, Phys. Rev. Lett. **99**, (2007) 192701.
3. C. L. Jiang *et al.*, Phys. Rev. C **79**, (2009) 044601.
4. C. H. Dasso and G. Pollarolo, Phys. Rev. C **39**, (1989) 2073.
5. L. Corradi, G. Pollarolo and S. Szilner, J. Phys. G: Nucl. Part. Phys. **36**, (2009) 113101.
6. M. Evers *et al.*, Phys. Rev. C **81**, (2010) 014602.
7. R. A. Broglia and A. Winther, *Heavy Ion Reactions (Lecture Notes), Volume 1: Elastic and Inelastic Reactions*, (The Benjamin/Cummings Publishing Company, Inc., 1981).
8. F. Videbaek *et al.*, Phys. Rev. C **15**, (1977) 954.
9. H. Timmers, *Expressions of inner freedom*, (PhD thesis, The Australian National University, 1996).
10. R. M. DeVries, *et al.*, Phys. Rev. Lett. **35**, (1975) 835.
11. H. Hasan and C. S. Warke, Nucl. Phys. A **318**, (1979) 523.
12. I. J. Thompson *el al.*, Nucl. Phys. A **505**, (1989) 84.
13. T. Tamura *et al.*, Phys. Rep. **65**, (1980) 345.
14. K.-H. Kim, T. Otsuka, and P. Bonche, J. Phys. G: Nucl. Part. Phys. **23**, (1997) 1267.
15. P. Bonche, H. Flocard, and P.H. Heenen, Nucl. Phys. A **467**,(1987) 115–135.
16. P. J. A. Buttle and L. J. B. Goldfarb, Nucl. Phys. A **176**, (1971) 299–320.
17. J. Wilczynski, Phys. Lett. B **47**, (1973) 124–128.
18. J. Wilczynski and H. W. Wilschut, Phys. Rev. C **39**, (1989) 2475–2476.
19. V. Zagrebaev and W. Greiner, J. Phys. G: Nucl. Part. Phys. **34**, (2007) 1–25.
20. C. L. Jiang *et al.*, Phys. Rev. C **75**, (2007) 015803.
21. L. R. Gasques *et al.*, Phys. Rev. C **76**, (2007) 035802.
22. C. Simenel, Phys. Rev. Lett. **105**, (2010) 192701.